JNC TN9400 2000-004

SIMMER-III Analytic Thermophysical Property Model

May 1999

O-arai Engineering Center
Japan Nuclear Cycle Development Institute

JNC TN9400 2000-004
May, 1 9 9 9

SIMMER-III Analytic Thermophysical Property Model

K. Morita* [a], Y. Tobita*, Sa. Kondo*
E. A. Fischer * [b]

Abstract

An analytic thermophysical property model using general function forms is developed for a reactor safety analysis code, SIMMER-III. The function forms are designed to represent correct behavior of properties of reactor-core materials over wide temperature ranges, especially for the thermal conductivity and the viscosity near the critical point. The most up-to-date and reliable sources for uranium dioxide, mixed-oxide fuel, stainless steel, and sodium available at present are used to determine parameters in the proposed functions. This model is also designed to be consistent with a SIMMER-III model on thermodynamic properties and equations of state for reactor-core materials.

* Fast Reactor Safety Engineering Group, Sodium and Safety Engineering Division
O-arai Engineering Center, JNC

a Present affiliation: Institute of Environmental Systems, Kyusyu University

b International Fellow
Present affiliation: Forschungszentrum Karlsruhe
Institut für Neutronenphysik und Reaktortechnik, Germany

JNC TN9400 2000-004
1 9 9 9 年 5 月

SIMMER-III 解析的熱物性モデル
(研究報告書)

守田　幸路*[a], 飛田　吉春*, 近藤　悟*
E. A. Fischer *[b]

要　旨

高速炉安全解析コードSIMMER-IIIに使用する解析的熱物性モデルを開発した。一般的な関数型を使用した本モデルは、広範囲の温度領域で炉心物質の熱物性の挙動、特に、臨界点近傍での熱伝導率と粘性を正しく表すように設計されている。二酸化ウラン、混合酸化物燃料、ステンレス鋼およびナトリウムについて、最新でかつ最も信頼できるデータを用いて提案した関数のパラメーターを決定した。本モデルは、SIMMER-IIIコードの炉心物質の熱力学的特性と状態方程式に関するモデルと整合性をもって設計されている。

*　大洗工学センター，ナトリウム・安全工学試験部，高速炉安全工学グループ
a　現所属　九州大学工学部付属　環境システム科学研究センター
b　国際特別研究員，現所属　独国カールスルーエ研究所

Contents

page

Abstract i

要 旨 ii

Contents iii

List of tables v

List of figures vi

Chapter 1. Introduction 1

Chapter 2. Analytic TPP model 2

2.1. Solid thermal conductivity 2

2.2. Thermal conductivity and viscosity of liquid and vapor phases 2

2.2.1. Simple function model 2

2.2.2. Extended function model 3

2.2.3. Theoretical model 4

2.2.4. Vapor mixture properties 5

2.3. Binary diffusion coefficient 6

2.4. Specific heat at constant pressure 7

2.5. Surface tension 8

2.6. Mechanical and adiabatic properties 8

Chapter 3. Properties of reactor materials 11

3.1. Solid thermal conductivity 11

A. Fuel 11

B. Stainless steel 11

3.2. Liquid thermal conductivity 11

A. Fuel 11

B. Stainless steel 12

C. Sodium 13

3.3. Liquid viscosity 13

A. Fuel 13

B. Stainless steel 13

C. Sodium 14

3.4. Vapor properties 14

A. Fuel 14

B. Stainless steel 15
C. Sodium........ 15

3.5. Surface tension........ 16
A. Fuel........ 16
B. Stainless steel 16
C. Sodium........ 19

3.6. Liquid heat capacity at constant pressure........ 20
A. Fuel........ 20
B. Stainless steel 20
C. Sodium........ 20

3.7. Code options and TPP functions........ 21

Chapter 4. Conclusions........ 22

Acknowledgments........ 23

Appendix A. Consistent formulation for thermal conductivity and viscosity........ 24

A.1. Review of Hanley's model........ 24

A.2. Proposed model 25

A.3. Application to water........ 27

Appendix B. Nomenclature 29

References........ 30

List of tables

page

Table 1. TPP functions for SIMMER-III.......... 33

Table 2. TPP parameters for fuel (UO_2).......... 34

Table 3. TPP parameters for fuel (MOX).......... 34

Table 4. TPP parameters for steel (type 316 stainless steel).......... 35

Table 5. TPP parameters for coolant (sodium).......... 35

List of figures

page

Fig. 1. Thermal conductivity of sodium 36

Fig. 2. Viscosity of sodium 36

Fig. 3. Surface forces in UO_2–stainless steel system 37

Fig. 4. Thermal conductivity of water 37

Fig. 5. Viscosity of water 38

Chapter 1. Introduction

Numerical simulation of postulated severe-accident sequences in liquid-metal fast reactors (LMFRs) requires thermodynamic properties of reactor-core materials such as fuel, steel, and coolant over wide temperature and pressure ranges. Especially, an accident analysis code like SIMMER-III (Kondo et al., 1992) requires the properties up to the critical point to complete an equation-of-state (EOS) model. In a series of two studies (Morita and Fischer, 1998; Morita et al., 1998), the thermodynamic properties and equations of state for the basic reactor-core materials have been successfully developed as a standard data basis for the fast reactor safety analysis. First, an improved analytic EOS model using flexible thermodynamic functions was newly developed for a multiphase, multicomponent fluid-dynamics code for LMFR safety analysis. This EOS model is designed to have adequate accuracy at high temperature and high pressure and to consistently satisfy basic thermodynamic relationships over a wide temperature range without deterioration of the computing efficiency. Second, thermodynamic properties of reactor-core materials were evaluated for the analytic EOS model, based on the new compilation of the most up-to-date and reliable sources. These EOS data completely satisfy the basic thermodynamic relationships among the EOS variables over the entire temperature ranges.

In this report, a complete set of analytical functions to calculate thermophysical properties is developed for use in the SIMMER-III code. This is called the analytic thermophysical property (TPP) model that provides thermal conductivity, viscosity, binary diffusion coefficient, surface tension, heat capacity, and mechanical and adiabatic properties with SIMMER-III models. The forms of the functions are not only taken from general formulas such as empirical equations and theoretical equations, but also newly designed to represent the dependency on major physical variables. For the thermal conductivity and viscosity, especially of sodium, improved formulation is newly proposed to represent the correct behavior of properties near the critical point. For fuel and steel, which have so high critical temperatures, properties in their vicinity should not become important in the reactor safety analysis. Therefore, a simple function model using polynomial and empirical equations as well as a model based on the kinetic theory of gases is also prepared to calculate the thermal conductivity and viscosity. Parameters in the proposed thermophysical functions are determined using most up-to-date and reliable sources for uranium dioxide, mixed-oxide fuel, stainless steel, and sodium. The present model can be used for the reactor safety analysis consistently with the previous studies on the thermodynamic properties and equation of state.

Chapter 2. Analytic TPP model

2.1. Solid thermal conductivity

The thermal conductivity is given for the structure components and solid particles in the liquid fields. The function for the structure thermal conductivity is expressed as a function of temperature:

$$\kappa_{\mathrm{Sm}} = a_{\mathrm{KS1,M}} + \frac{a_{\mathrm{KS2,M}}}{T_{\mathrm{Sm}}} + \frac{a_{\mathrm{KS3,M}}}{T_{\mathrm{Sm}}{}^2} + a_{\mathrm{KS4,M}} T_{\mathrm{Sm}} + a_{\mathrm{KS5,M}} T_{\mathrm{Sm}}{}^2, \tag{1}$$

where $a_{\mathrm{KS1,M}}$, $a_{\mathrm{KS2,M}}$, $a_{\mathrm{KS3,M}}$, $a_{\mathrm{KS4,M}}$, and $a_{\mathrm{KS5,M}}$ are fitting constants. This function is applied over the whole solid temperature range. The same function as the structure is used for a solid particle component as well.

The thermal conductivity of solid fuel decreases with increasing porosity. Harding et al. (1989) proposed that the following formula be used to correct for this porosity effect over a range of porosity of practical interest:

$$\kappa_{\mathrm{Sm}}^{\mathrm{P}} = \kappa_{\mathrm{Sm}} (1 - \varepsilon_{\mathrm{Sm}})^{2.5}, \tag{2}$$

where $\varepsilon_{\mathrm{Sm}}$ is the fractional porosity of solid fuel and $\kappa_{\mathrm{Sm}}^{\mathrm{P}}$ is the corresponding thermal conductivity. Equation (2) is employed to take into account the porosity effect on the thermal conductivity of solid fuel.

2.2. Thermal conductivity and viscosity of liquid and vapor phases

2.2.1. Simple function model

The simple function model to calculate liquid properties uses a quadratic equation for the thermal conductivity, and the Andrade equation for the viscosity. The expression for the thermal conductivity is

$$\kappa_{\mathrm{Lm}} = a_{\mathrm{KL1,M}} + a_{\mathrm{KL2,M}} T_{\mathrm{Lm}} + a_{\mathrm{KL3,M}} T_{\mathrm{Lm}}{}^2, \tag{3}$$

where $a_{\mathrm{KL1,M}}$, $a_{\mathrm{KL2,M}}$, and $a_{\mathrm{KL3,M}}$ are fitting constants. For the viscosity,

$$\mu_{\mathrm{Lm}} = b_{\mathrm{ML1,M}} \exp\left(\frac{b_{\mathrm{ML2,M}}}{T_{\mathrm{Lm}}} \right), \tag{4}$$

where $b_{\mathrm{ML1,M}}$ and $b_{\mathrm{ML2,M}}$ can be fit or taken directly from the available database. Constant values of the properties at the critical point are simply used in the temperature range above the critical point.

If properties of a vapor component are known by experimental data or other reliable sources, simple functions can be used as a function of temperature. The formula for the thermal conductivity is taken from the empirical equation of fuel thermal conductivity (Frurip and Fink, 1982), and a quadratic equation is used for the viscosity. The expression for the thermal conductivity is

$$\kappa_{\mathrm{Gm}} = \exp(a_{\mathrm{KG1,M}} + \frac{a_{\mathrm{KG2,M}}}{T_{\mathrm{G}}} + a_{\mathrm{KG3,M}}T_{\mathrm{G}} + a_{\mathrm{KG4,M}}T_{\mathrm{G}}^{2} + a_{\mathrm{KG5,M}}T_{\mathrm{G}}^{3}), \tag{5}$$

where $a_{\mathrm{KG1,M}}$, $a_{\mathrm{KG2,M}}$, $a_{\mathrm{KG3,M}}$, $a_{\mathrm{KG4,M}}$, and $a_{\mathrm{KG5,M}}$ are fitting constants. For the viscosity,

$$\mu_{\mathrm{Gm}} = b_{\mathrm{MG1,M}} + b_{\mathrm{MG2,M}}T_{\mathrm{G}} + b_{\mathrm{MG3,M}}T_{\mathrm{G}}^{2}, \tag{6}$$

where $b_{\mathrm{MG1,M}}$, $b_{\mathrm{MG2,M}}$, and $b_{\mathrm{MG3,M}}$ are fitting constants. An upper limit of the vapor temperature range allowed in Eqs. (5) and (6) is specified by an input maximum vapor temperature, $T_{\mathrm{Gmax,M}}$, which determines maximum values of the properties.

2.2.2. *Extended function model*

The extended function model for the calculation of liquid and vapor properties uses formulas consistent in the vicinity of the critical point and treats dependence of vapor properties on density and temperature (Appendix A). The formulas give the correct behavior of the properties, that is, the increase of the vapor viscosity and thermal conductivity due to increased density near the critical point. For the liquid properties, the simple analytical functions are replaced near the critical point with an additional equation so as to represent an infinite slope and a value consistent with the vapor phase at the critical point. The proposed formula for the liquid thermal conductivity is

$$\kappa_{\mathrm{Lm}} = a_{\mathrm{KL1,M}} + a_{\mathrm{KL2,M}}T_{\mathrm{Lm}} + a_{\mathrm{KL3,M}}T_{\mathrm{Lm}}^{2}, \qquad T_{\mathrm{Lm}} \le a_{\mathrm{SL4,M}}T_{\mathrm{Crt,M}}, \tag{7a}$$

$$\kappa_{\mathrm{Lm}} = \kappa_{\mathrm{Crt,M}} + a_{\mathrm{KL5,M}}(T_{\mathrm{Crt,M}} - T_{\mathrm{Lm}})^{1/2} + a_{\mathrm{KL6,M}}(T_{\mathrm{Crt,M}} - T_{\mathrm{Lm}})^{2}, \tag{7b}$$

$$a_{\mathrm{SL4,M}}T_{\mathrm{Crt,M}} < T_{\mathrm{Lm}} \le T_{\mathrm{Crt,M}}, \text{ and}$$

$$\kappa_{\mathrm{Lm}} = \kappa_{\mathrm{Crt,M}}, \qquad T_{\mathrm{Lm}} > T_{\mathrm{Crt,M}}, \tag{7c}$$

where $a_{\mathrm{KL1,M}}$, $a_{\mathrm{KL2,M}}$, $a_{\mathrm{KL3,M}}$, $a_{\mathrm{KL4,M}}$, $a_{\mathrm{KL5,M}}$, and $a_{\mathrm{KL6,M}}$ are fitting constants. For the liquid viscosity,

$$\mu_{\mathrm{Lm}} = b_{\mathrm{ML1,M}} \exp\left(\frac{b_{\mathrm{ML2,M}}}{T_{\mathrm{Lm}}}\right), \qquad T_{\mathrm{Lm}} \le b_{\mathrm{ML3,M}}T_{\mathrm{Crt,M}}, \tag{8a}$$

$$\mu_{\mathrm{Lm}} = \mu_{\mathrm{Crt,M}} + b_{\mathrm{ML4,M}}(T_{\mathrm{Crt,M}} - T_{\mathrm{Lm}})^{1/2} + b_{\mathrm{ML5,M}}(T_{\mathrm{Crt,M}} - T_{\mathrm{Lm}})^{2}, \tag{8b}$$

$$b_{\mathrm{ML3,M}} T_{\mathrm{Crt,M}} < T_{\mathrm{Lm}} \le T_{\mathrm{Crt,M}}, \text{ and}$$

$$\mu_{\mathrm{Lm}} = \mu_{\mathrm{Crt,M}}, \qquad T_{\mathrm{Lm}} > T_{\mathrm{Crt,M}}, \tag{8c}$$

where $b_{\mathrm{ML1,M}}$, $b_{\mathrm{ML2,M}}$, $b_{\mathrm{ML3,M}}$, $b_{\mathrm{ML4,M}}$, and $b_{\mathrm{ML5,M}}$ are fitting constants.

For the vapor phase, the properties are assumed to depend on the density and the temperature and are calculated by a simple power function up to the critical temperature and a constant values beyond it. The value above the critical temperature is made consistent with the liquid-side equations at the critical point. The formula for the vapor thermal conductivity is

$$\kappa_{\mathrm{Gm}} = \kappa_{\mathrm{Gm}}^{\mathrm{D}} + [\kappa_{\mathrm{Crt.M}} - \kappa_{\mathrm{Gm}}^{\mathrm{D}}(T_{\mathrm{Crt.M}})]\left(\frac{T_{\mathrm{G}}}{T_{\mathrm{Crt.M}}}\right)^{n_{f,M}} \frac{v_{\mathrm{Crt.M}}}{v_{\mathrm{Gm}}}, \tag{9a}$$

$$T_{\mathrm{G}} \le T_{\mathrm{Crt,M}}, \text{ and}$$

$$\kappa_{\mathrm{Gm}} = \kappa_{\mathrm{Crt,M}}, \qquad T_{\mathrm{G}} > T_{\mathrm{Crt,M}}, \tag{9b}$$

where $n_{f,M}$ is a fitting constant, and $\kappa_{\mathrm{Gm}}^{\mathrm{D}}$ refers to the thermal conductivity of the dilute gas and is expressed by a linear equation as a function of temperature:

$$\kappa_{\mathrm{Gm}}^{\mathrm{D}} = a_{\mathrm{KG1,M}} + a_{\mathrm{KG2,M}} T_{\mathrm{G}}, \tag{10}$$

where $a_{\mathrm{KG1,M}}$ and $a_{\mathrm{KG2,M}}$ are fitting constants. For the viscosity,

$$\mu_{\mathrm{Gm}} = \mu_{\mathrm{Gm}}^{\mathrm{D}} + [\mu_{\mathrm{Crt.M}} - \mu_{\mathrm{Gm}}^{\mathrm{D}}(T_{\mathrm{Crt.M}})]\left(\frac{T_{\mathrm{G}}}{T_{\mathrm{Crt.M}}}\right)^{n_{f,M}} \frac{v_{\mathrm{Crt.M}}}{v_{\mathrm{Gm}}}, \tag{11a}$$

$$T_{\mathrm{G}} \le T_{\mathrm{Crt,M}}, \text{ and}$$

$$\mu_{\mathrm{Gm}} = \mu_{\mathrm{Crt,M}}, \qquad T_{\mathrm{G}} > T_{\mathrm{Crt,M}}, \tag{11b}$$

where $\mu_{\mathrm{Gm}}^{\mathrm{D}}$ refers to the viscosity of the dilute gas and is also expressed by a linear equation as a function of temperature:

$$\mu_{\mathrm{Gm}}^{\mathrm{D}} = b_{\mathrm{MG1,M}} + b_{\mathrm{MG2,M}} T_{\mathrm{G}}, \tag{12}$$

where $b_{\mathrm{MG1,M}}$ and $b_{\mathrm{MG2,M}}$ are fitting constants.

2.2.3. Theoretical model

In the theoretical model, the vapor properties can be calculated using the Chapman-Enskog kinetic theory of gases and the Lennard-Jones model for the potential energy of interaction (Bird et al., 1960; Chawla et al., 1981; Reid et al., 1988). The viscosity is given by

$$\mu_{\mathrm{Gm}} = 2.6993\times10^{-6}\frac{\sqrt{W_{\mathrm{M}}T_{\mathrm{G}}}}{\sigma_{\mathrm{M}}{}^{2}\Omega_{\mathrm{k,m}}}, \tag{13}$$

where σ_{M} is the Lennard-Jones collision diameter in angstrom units and the parameter, $\Omega_{\mathrm{k,m}}$, is called collision integral as a function of the vapor temperature. An empirical equation for $\Omega_{\mathrm{k,m}}$ was proposed by Neufeld et al. (1972):

$$\Omega_{\mathrm{k,m}} = [A(T^*)^{-B}] + C[\exp(-DT^*)] + E[\exp(-FT^*)], \tag{14}$$

where $T^* = k_{\mathrm{B}}T_{\mathrm{G}}/\varepsilon_{\mathrm{M}}$, A = 1.16145, B = 0.14874, C = 0.52487, D = 0.77320, E = 2.16178, and F = 2.43787, and k_{B} is Boltzmann's constant. Equation (14) is applicable from $0.3 \le T^* \le 100$ with an average deviation of only 0.064 %. In SIMMER-III, the Lennard-Jones parameters, σ_{M} and $\varepsilon_{\mathrm{M}}/k_{\mathrm{B}}$, are treated as input constants of material M.

For monatomic gases, the thermal conductivity is given by

$$\kappa_{\mathrm{Gm}} = \frac{5}{2}c_{\mathrm{v,Gm}}\mu_{\mathrm{Gm}}, \tag{15}$$

where $c_{\mathrm{v,Gm}}$, is the vapor heat capacity at constant volume, and is calculated by the EOS function. For polyatomic gases, with the use of a modified Eucken correction, the thermal conductivity is given by

$$\kappa_{\mathrm{Gm}} = (1.32c_{\mathrm{v,Gm}} + 1.77R_{\mathrm{M}})\mu_{\mathrm{Gm}}. \tag{16}$$

where R_m is the gas constant.

2.2.4. *Vapor mixture properties*

To calculate the exchange functions involving the vapor field, the average thermal conductivity and viscosity of the vapor mixture are required. Chawla et al. (1981) used the following semi-empirical formulas of Wilke (1950) for the properties of a vapor mixture:

$$\mu_{\mathrm{G}} = \sum_{i=1}^{\mathrm{MCGM1}} \frac{x_i\mu_{\mathrm{G}i}}{\sum_{j=1}^{\mathrm{MCGM1}} x_j\phi_{ij}}, \text{ and} \tag{17}$$

$$\kappa_{\mathrm{G}} = \sum_{i=1}^{\mathrm{MCGM1}} \frac{x_i\kappa_{\mathrm{G}i}}{\sum_{j=1}^{\mathrm{MCGM1}} x_j\phi_{ij}}, \tag{18}$$

where MCGM1 is the number of vapor components in the mixture,

$$\phi_{ij} = \frac{\left[1+\left(\frac{\mu_{Gi}}{\mu_{Gj}}\right)^{1/2}\left(\frac{W_{M(Gj)}}{W_{M(Gi)}}\right)^{1/4}\right]}{2\sqrt{2}\left(1+\frac{W_{M(Gj)}}{W_{M(Gi)}}\right)^{1/2}}, \tag{19}$$

x_i is the mole fraction of a component i in the mixture, and is related to the specific volume, υ_{Gi}, through the relation

$$x_i = \frac{\frac{1}{\upsilon_{Gi}W_{M(Gi)}}}{\sum_{j=1}^{MCGMI}\frac{1}{\upsilon_{Gj}W_{M(Gj)}}}. \tag{20}$$

2.3. Binary diffusion coefficient

The diffusion coefficient for a binary system is calculated from the Chapman-Enskog theory assuming the potential between the molecules is represented by the Lennard-Jones type (Reid et al., 1988). The binary diffusion coefficient for species i and j is expressed as

$$D_{ij} = \frac{3}{16}\frac{\sqrt{4\pi k_B \frac{1}{2}\left(\frac{1}{W_{M(Gi)}}+\frac{1}{W_{M(Gj)}}\right)}}{n\pi\sigma_{ij}^2\Omega_D}f_D, \tag{21}$$

where is n the number density of molecules in the mixture, σ_{ij} is the Lennard-Jones collision diameter for diffusion in angstrom units, f_D is a correction factor close to unity, and Ω_D is the collision integral for diffusion as a function of the vapor temperature. An empirical equation for Ω_D was proposed by Neufeld et al. (1972):

$$\Omega_D = [A(T^*)^{-B}] + C[\exp(-DT^*)] + E[\exp(-FT^*)] + G[\exp(-HT^*)], \tag{22}$$

where $T^* = k_B T_G/\varepsilon_{ij}$, A = 1.06036, B = 0.15610, C = 0.19300, D = 0.47635, E = 1.03587, F = 1,52996, G = 1.76474, and H = 3.89411. The values of ε_{ij} and σ_{ij} are obtained by combining the Lennard-Jones parameters of species i and j empirically:

$$\sigma_{ij} = \frac{1}{2}(\sigma_{M(Gi)} + \sigma_{M(Gj)}), \text{ and} \tag{23}$$

$$\varepsilon_{ij} = (\varepsilon_{M(Gi)}\varepsilon_{M(Gj)})^{1/2}. \tag{24}$$

We use the following simplified expression of Eq. (21) assuming that f_D is chosen as unity and n is expressed by the ideal gas law:

$$D_{ij} = 2.66 \times 10^{-2} \frac{T_G^{\ 3/2} \sqrt{\dfrac{1}{2}\left(\dfrac{1}{W_{\mathrm{M(G}i)}} + \dfrac{1}{W_{\mathrm{M(G}j)}}\right)}}{(p_{\mathrm{G}i} + p_{\mathrm{G}j})\sigma_{ij}^{\ 2}\Omega_{\mathrm{D}}} . \tag{25}$$

The diffusion coefficient in multicomponent gas systems is simply defined by an effective binary diffusivity D_{im} for the diffusion of i in a mixture (Bird et al., 1960). We use the following formula for D_{im} expressed as the effective diffusion coefficient of i with respect to a multicomponent mixture of stagnant gases (Wilke, 1950):

$$D_{im} = (1 - x_i)\left(\sum_{\substack{j=1 \\ j \neq i}}^{n} \frac{x_j}{D_{ij}}\right)^{-1} . \tag{26}$$

2.4. Specific heat at constant pressure

The liquid heat capacity at constant pressure can be evaluated using EOS functions based on thermodynamic relationships. However, it was found that this poorly reproduces the sodium heat capacity in the temperature range where the experimental data are well developed. This is due to simplification assumed in the modified Redlich-Kwong (MRK) equation extended to a reacting system by Morita and Fischer (1998), although this equation provides an improved description of thermodynamic states of sodium vapor, which cannot be obtained by the MRK equation for a single component. The liquid heat capacity at constant pressure is used to calculate Prandtl number in Nusselt number correlations and hence it is not necessary for a TPP function to consistently satisfy thermodynamic relationships among state variables. We use the following polynomial function form to fit liquid heat capacity data:

$$c_{\mathrm{p,Lm}} = f(\eta_{\mathrm{Lm}})^{-1}, \tag{27}$$

where

$$f(\eta_{\mathrm{Lm}}) = d_{\mathrm{CL1,M}}(1-\eta_{\mathrm{Lm}}) + d_{\mathrm{CL2,M}}(1-\eta_{\mathrm{Lm}})^{3/2} + d_{\mathrm{CL3,M}}(1-\eta_{\mathrm{Lm}})^2$$

$$+ d_{\mathrm{CL4,M}}(1-\eta_{\mathrm{Lm}})^3 + d_{\mathrm{CL5,M}}(1-\eta_{\mathrm{Lm}})^4 + d_{\mathrm{CL6,M}}(1-\eta_{\mathrm{Lm}})^5, \tag{28}$$

and $\eta_{\mathrm{Lm}} = \dfrac{T_{\mathrm{Lm}}}{T_{\mathrm{Crt,M}}}$. An upper limit of liquid heat capacity is specified by an input parameter, $c_{\mathrm{pLmax,M}}$, of which default value is 10^4 J kg^{-1} K^{-1}.

The vapor heat capacity at constant pressure is evaluated using the thermodynamic relationship:

$$c_{\mathrm{p,Gm}} = c_{\mathrm{v,Gm}} - \frac{T_{\mathrm{G}}\left(\dfrac{\partial p_{\mathrm{Gm}}}{\partial T_{\mathrm{G}}}\right)^2_{v_{\mathrm{Gm}}}}{\left(\dfrac{\partial p_{\mathrm{Gm}}}{\partial v_{\mathrm{Gm}}}\right)_{T_{\mathrm{G}}}}. \tag{29}$$

An upper limit of vapor heat capacity is specified by an input parameter, $c_{\mathrm{pGmax,M}}$, of which default value is 10^4 J kg^{-1} K^{-1}. The values of $\left(\dfrac{\partial e_{\mathrm{Gm}}}{\partial T_{\mathrm{G}}}\right)_{v_{\mathrm{Gm}}}$, $\left(\dfrac{\partial p_{\mathrm{Gm}}}{\partial T_{\mathrm{G}}}\right)_{v_{\mathrm{Gm}}}$, and $\left(\dfrac{\partial p_{\mathrm{Gm}}}{\partial v_{\mathrm{Gm}}}\right)_{T_{\mathrm{G}}}$ are obtained from the EOS functions. The heat capacity of the vapor mixture is defined by the derivative of the specific internal energy of the vapor mixture with respect to the vapor temperature:

$$c_{\mathrm{p,G}} = \frac{\sum_{\mathrm{m=1}}^{\mathrm{MCGMI}} v_{\mathrm{Gm}} c_{\mathrm{p,Gm}}}{\sum_{\mathrm{m=1}}^{\mathrm{MCGMI}} v_{\mathrm{Gm}}}. \tag{30}$$

2.5. Surface tension

Since the interface between liquid and gas phase disappears at the critical temperature, the surface tension of liquid is reduced to zero at the critical temperature and decreases with increasing temperature. The general form of the surface tension is given by the van der Waals equation:

$$\sigma_{\mathrm{Lm}} = c_{\mathrm{SL1,M}}\left(1 - \frac{T_{\mathrm{Lm}}}{T_{\mathrm{Crt,M}}}\right)^{c_{\mathrm{SL2,M}}}, \tag{31}$$

where $c_{\mathrm{SL1,M}}$ and $c_{\mathrm{SL2,M}}$ are fitting constants. The minimum value of the surface tension can be specified by an input parameter $c_{\mathrm{SL3,M}}$ to avoid numerical difficulties. Equation (31) is fit to the data of surface tension when in contact with a third gas or vapor phase. The surface tension of between two immiscible liquid phases Lm and Lm' is calculated by

$$\sigma_{\mathrm{Lm,Lm'}} = \sigma_{\mathrm{Lm}} + \sigma_{\mathrm{Lm'}} - 2(\sigma_{\mathrm{Lm}}\sigma_{\mathrm{Lm'}})^{1/2}. \tag{32}$$

Although this relation is strictly appropriate to nonpolar materials, Eq. (32) is usually a good approximation for the case where either Lm and Lm' is nonpolar (Carey, 1992).

2.6. Mechanical and adiabatic properties

Solving the following thermodynamic relationships for the volumetric thermal expansion coefficient $\alpha_{\mathrm{p,Lm}}$ and the isothermal compressibility $\beta_{\mathrm{T,Lm}}$,

$$c_{v,Lm} = c_{p,Lm} - \frac{T_{Lm} v_{Lm} \alpha_{p,Lm}{}^2}{\beta_{T,Lm}}, \tag{33}$$

$$\left(\frac{\partial T_{Lm}}{\partial p}\right)_{e_{Lm}} = \left\{ \frac{\alpha_{p,Lm}}{\beta_{T,Lm}} + \frac{c_{v,Lm}}{v_{Lm}\beta_{T,Lm}(T_{Lm}\dfrac{\alpha_{p,Lm}}{\beta_{T,Lm}} - p)} \right\}^{-1}, \text{ and} \tag{34}$$

$$\left(\frac{\partial v_{Lm}}{\partial p}\right)_{e_{Lm}} = \left\{ -\frac{1}{v_{Lm}\beta_{T,Lm}} - \frac{T_{Lm}\dfrac{\alpha_{p,Lm}}{\beta_{T,Lm}} - p}{c_{v,Lm}} \frac{\alpha_{p,Lm}}{\beta_{T,Lm}} \right\}^{-1}, \tag{35}$$

we obtain the following expressions for $\alpha_{p,Lm}$ and $\beta_{T,Lm}$:

$$\alpha_{p,Lm} = \frac{1}{v_{Lm} T_{Lm}} \left[c_{p,Lm} \left(\frac{\partial T_{Lm}}{\partial p}\right)_{e_{Lm}} - p \left(\frac{\partial v_{Lm}}{\partial p}\right)_{e_{Lm}} \right], \text{ and} \tag{36}$$

$$\beta_{T,Lm} = \frac{1}{v_{Lm}} \left\{ \frac{1}{T_{Lm}} \left(\frac{\partial T_{Lm}}{\partial p}\right)_{e_{Lm}} \left[c_{p,Lm} \left(\frac{\partial T_{Lm}}{\partial p}\right)_{e_{Lm}} - p \left(\frac{\partial v_{Lm}}{\partial p}\right)_{e_{Lm}} \right] - \left(\frac{\partial v_{Lm}}{\partial p}\right)_{e_{Lm}} \right\}. \tag{37}$$

For the adiabatic compressibility $\beta_{S,Lm}$ and the speed of sound $v_{S,Lm}$, using the following well-known thermodynamic relationships,

$$c_{v,Lm} = \frac{\beta_{S,Lm}}{\beta_{T,Lm}} c_{p,Lm}, \text{ and} \tag{38}$$

$$\beta_{S,Lm} = \frac{v_{Lm}}{v_{S,Lm}^2}, \tag{39}$$

we can write

$$\beta_{S,Lm} = \frac{1}{v_{Lm}} \left(\frac{\partial v_{Lm}}{\partial p}\right)_{e_{Lm}} \left\{ \frac{p}{T_{Lm}} \left[\left(\frac{\partial T_{Lm}}{\partial p}\right)_{e_{Lm}} - \frac{p}{c_{p,Lm}} \left(\frac{\partial v_{Lm}}{\partial p}\right)_{e_{Lm}} \right] - 1 \right\}, \text{ and} \tag{40}$$

$$v_{S,Lm} = v_{Lm} \left(\frac{\partial v_{Lm}}{\partial p}\right)_{e_{Lm}} \left\{ \frac{p}{T_{Lm}} \left[\left(\frac{\partial T_{Lm}}{\partial p}\right)_{e_{Lm}} - \frac{p}{c_{p,Lm}} \left(\frac{\partial v_{Lm}}{\partial p}\right)_{e_{Lm}} \right] - 1 \right\}^{-1/2}. \tag{41}$$

For these liquid properties along the saturation curve, Eqs. (36), (37), (40), and (41) can be calculated using the EOS functions developed in our previous study (Morita and Fischer, 1998).

For vapor phase, the volumetric thermal expansion coefficient $\alpha_{p,Gm}$, the isothermal compressibility $\beta_{T,Gm}$, and the adiabatic compressibility $\beta_{S,Gm}$ are expressed by

$$\alpha_{p,Gm} = -\frac{1}{v_{Gm}} \frac{\left(\dfrac{\partial p_{Gm}}{\partial T_G}\right)_p}{\left(\dfrac{\partial p_{Gm}}{\partial v_{Gm}}\right)_{T_G}}, \tag{42}$$

$$\beta_{T,Gm} = -\frac{1}{v_{Gm}} \left(\frac{\partial p_{Gm}}{\partial v_{Gm}}\right)_{T_G}^{-1}, \text{ and} \tag{43}$$

$$\beta_{S,Gm} = \beta_{T,Gm} \frac{c_{v,Gm}}{c_{p,Gm}}. \tag{44}$$

These are also calculated using the EOS functions with the MRK equations for vapor phase.

Chapter 3. Properties of reactor materials

3.1. Solid thermal conductivity

A. Fuel

For solid mixed oxide fuel, $(U_{0.8}Pu_{0.2})O_{1.98}$, with 95 % TD, Philipponneau (1992) obtained the following empirical correlation:

$$\kappa = \frac{1}{0.1562 + 2.885 \times 10^{-4} T} + 76.38 \times 10^{-12} T^3, \qquad 500\ \mathrm{K} < T < T_\mathrm{m}, \tag{45}$$

where κ is in W m^{-1} K^{-1} and T is in K. The thermal conductivity of fully dense solid $(U_{0.8}Pu_{0.2})O_{1.98}$ is evaluated using Eq. (2) with the value of fractional porosity, 0.05.

For fully dense solid UO_2, Fink and Petri (1997) recommended the following equation of Harding and Martin (1989), which was derived for the temperature range of 773 K to the melting point, 3120 K:

$$\kappa = \frac{1}{0.0375 + 2.165 \times 10^{-4} T} + \frac{4.715 \times 10^{9}}{T^2} \exp\left(-\frac{16361}{T}\right), \tag{46}$$

where κ is in W m^{-1} K^{-1} and T is in K. Fink and Petri stated that this equation is in good agreement with other ones that fit the experimental data below 773 K.

B. Stainless steel

Harding et al. (1989) recommended the following correlation for the thermal conductivity of type 316 stainless steel in solid state below their recommended solidus temperature (= 1683 K):

$$\kappa = 9.735 + 0.1434 \times 10^{-1} T, \tag{47}$$

where κ is in W m^{-1} K^{-1} and T is in K. This equation is used over the whole solid temperature range.

3.2. Liquid thermal conductivity

A. Fuel

No thermal conductivity data have been reported for molten mixed oxide fuel. For liquid UO_2, only four measurements are available. Kim et al. (1977) used a modulated electron beam technique to measure the thermal diffusivity of molten UO_2 clad in tungsten in the temperature range of 3187 to 3310 K. Their recommended value for the thermal conductivity at the melting point is 11 W m^{-1} K^{-1}. Otter and Damien (1984) measured the thermal diffusivity of molten UO_2 contained in tungsten using a laser flash method in the temperature range of 3133 to 3273 K.. Their reported value for the thermal conductivity is 8.5 $W m^{-1} K^{-1}$. Tasman et al. (1983) obtained the thermal conductivity of molten UO_2 just above its melting point from a quasi-stationary method on a partially molten, self-contained sample. They obtained 2.2±1.0 $W m^{-1} K^{-1}$ from determination of the depth of a molten layer of a UO_2 cylinder. Fink and Leibowitz (1985) performed an analysis of the above three measurements of the thermal conductivity and thermal diffusivity of molten UO_2 using a transient heat transfer code. They found a much smaller range of values for thermal conductivity than originally reported: the original values ranged from 2.4 to 11 $W m^{-1} K^{-1}$ with a mean of 7.3 W/m/K, whereas the recalculated values ranged from 4.5 to 6.75 $W m^{-1} K^{-1}$ with a mean value of 5.6 $W m^{-1} K^{-1}$. Tasman (1989) performed a measurement of the thermal conductivity of liquid UO_2 using a rapid 2D temperature-scanning device and included unsteady transport in the 2D finite-element-method analysis, confirming his previous measurements (Tasman et al., 1983). According to Ronchi et al. (1993), Tasman obtained an average thermal conductivity of 2.5 ± 1 $W m^{-1} K^{-1}$ just above the melting point, which is lower than the solid conductivity at the melting point. Tasman also suggested that the discrepancy with the results of other authors, obtained on molten UO_2 contained in tungsten capsules, is due to the dissolution of tungsten in UO_2 samples at the melting point of the latter.

Recently, Fink and Petri (1997) recommended the thermal conductivity of liquid UO_2 in the range of 2.5 to 3.6 $W m^{-1} K^{-1}$, based on a detailed review of the above limited data. The lower limit is the new value reported by Tasman (1988) and the upper limit is consistent with the lower value obtained from the experiment by Kim et al. (1977) with the optically thick radiative contribution subtracted. Here, a mean value of the range recommended by Fink and Petri (1997) is used:

$$\kappa = 3.15\ \mathrm{W\,m^{-1}\,K^{-1}}. \tag{48}$$

For the thermal conductivity of liquid fuel, we use the simple function model and the above value is used over the whole liquid temperature range.

B. Stainless steel

For the type 316 stainless steel in liquid state, Harding et al. (1989) recommended the following correlation:

$$\kappa = 10.981 + 3.214\times10^{-3}T, \qquad T_m \le T \le 2073\ \mathrm{K}, \tag{49}$$

where κ is in $W m^{-1} K^{-1}$ and T is in K. For the thermal conductivity of liquid stainless steel, we use the simple function model and this equation is used over the whole liquid temperature range.

C. Sodium

For the calculation of the thermal conductivity of liquid sodium, Fink and Leibowitz (1996) recommended the following equation

$$\kappa = 124.67 - 0.11381T + 5.5226\times10^{-5}T^2 - 1.1842\times10^{-8}T^3, \qquad (50)$$

where κ is in W m^{-1} K^{-1} and T is in K. This equation is a least squares fit to data obtained from measurements in the temperature range 371-1500 K and is consistent with the thermal conductivity of the vapor at the critical point. They used the value of 0.052 W m^{-1} K^{-1} at the critical point, which was obtained from extrapolation of the values for the thermal conductivity of sodium vapor recommended by Vargaftik and Yargin (1985) in their review of experimental data and calculations of transport processes for alkali-metal vapors. It is noted that this critical value is significantly lower than the other evaluations, 1.8 W m^{-1} K^{-1} by Bystrov et al. (1990) and 5 W m^{-1} K^{-1} by Thurnay (1981).

The thermal conductivity of liquid sodium is calculated using the extended function model. Equation (7a) is fitted to the values calculated by Eq. (50) from the melting point to 2500 K, and then Eqs. (8a) and (8b) are connected at 2000 K. The value of 5.16 W m^{-1} K^{-1} is used as the thermal conductivity at the critical point, which is evaluated from the Wiedemann-Franz-Lorentz law formerly used by Fink and Leibowitz (1982), instead of their new recommendation in 1996. This is because the value of 0.052 W m^{-1} K^{-1} is inconsistent with the fact that the vapor thermal conductivity increases near the critical point, and is too low to reasonably fit the extended function, Eq. (9a), to sodium vapor. In Fig. 1, the thermal conductivity of liquid sodium calculated by the extended function model is shown, together with the recommendation by Fink and Leibowitz (1996).

3.3. Liquid viscosity

A. Fuel

No viscosity measurement has been reported for molten mixed oxide fuels. For liquid UO_2, Fink and Petri (1997) recommended Woodley's results (1974) represented by the relation:

$$\mu = 0.988\times10^{-3}\exp\left(\frac{4620}{T}\right), \qquad 3143 \le T \le 3303\text{ K}. \qquad (51)$$

where μ is in Pa s and T is in K. For the liquid fuel viscosity, we use the simple function model and hence the parameters in Eq. (4) are taken directly from Eq. (51).

B. Stainless steel

No viscosity measurements have been reported for the liquid stainless steel of type 316.

According to Bober et al. (1983), the viscosity of liquid stainless steel of type 1.4970 is expressed by

$$\mu = 2.93\times10^{-5}\exp\left(\frac{9715}{T}\right), \tag{52}$$

where μ is in Pa s and T is in K. For stainless steel, we use the simple function model and this equation is directly used over the whole liquid temperature range.

C. Sodium

Fink and Leibowitz (1996) recommended the following equation by Shpil'rain et al. (1965) to calculate the viscosity of liquid sodium for the temperature range 371 to 2500 K:

$$\ln\mu = -6.4406 - 0.3958\ln T + \frac{556.835}{T}, \tag{53}$$

where μ is in Pa s and T is in K. Fink and Leibowitz also recommended the critical value of the sodium viscosity by Bystrov et al. (1990):

$\mu_{Crt} = 5.8\times10^{-5}$ Pa s.

The viscosity of liquid sodium is calculated using the extended function model. Equation (8a) is fitted to the values calculated by Eq. (53) from the melting point to 2500 K and Eqs. (8a) and (8b) are connected at 2000 K. In Fig. 2, the viscosity of liquid sodium calculated by the extended function model is shown, together with the recommendation by Fink and Leibowitz.

3.4. Vapor properties

A. Fuel

No thermal conductivity data have been reported for mixed oxide fuel vapor. Frurip and Fink (1982) theoretically evaluated the thermal conductivity of a saturated vapor of $UO_{1.98}$ over the temperature range 3000 - 6000 K and recommended the following empirical equation:

$$\kappa = \exp\left(a + \frac{b}{T} + cT + dT^2 + eT^3\right), \tag{54}$$

where κ is in cal cm^{-1} s^{-1} K^{-1}, $a = 268.90$, $b = -3.1919\times10^5$, $c = -8.9673\times10^{-2}$, $d = 1.2861\times10^{-5}$, and $e = -6.7917\times10^{-10}$. For the thermal conductivity of fuel vapor, we use the simple analytical function and hence the parameters in Eq. (5) are taken directly from Eq. (54).

The vapor viscosity is calculated by the theoretical model using the following Leonard-Jones parameters (Frurip and Fink, 1982):

$\varepsilon_{\mathrm{M}}/k_{\mathrm{B}} = 5694$ K, and

$\sigma_{\mathrm{M}} = 4.03$ Å.

B. Stainless steel

No thermal conductivity and viscosity measurements have been reported for steel vapor. Chawla et al. (1981) calculated the thermal conductivity based on the Chapman-Enskog kinetic theory using the heat capacity which includes the effect of electric excitation by considering iron as the dominant component. They suggested that the contribution of electric excitation to the thermal conductivity, though small at low temperature, should become significant in a high temperature range as well as the heat capacity. In the EOS model, however, the modified Redlich-Kwong EOS cannot describe the contribution of electronic excitation to the steel vapor. Therefore, we employ values of the thermal conductivity calculated by Chawla et al. (1981), which were obtained by considering steel as a monatomic vapor, to fit Eq. (5) for the simple function model.

The vapor viscosity is calculated by the theoretical model using the following Leonard-Jones parameters (Chawla et al., 1981):

$\varepsilon_{\mathrm{M}}/k_{\mathrm{B}} = 3264$ K, and

$\sigma_{\mathrm{M}} = 2.414$ Å.

C. Sodium

The thermal conductivity and viscosity of sodium vapor are calculated using the extended function model. The reference values as dilute gas are taken from the data of saturated sodium vapor from 700 K to 1500 K recommended by Vargaftik and Yargin (1985), and hence Eqs. (10) and (12) are fitted to their data. For the value of $n_{\mathrm{r,M}}$, we apply $n_{\mathrm{r,M}} = 1$ which gives better consistency with the evaluation of the sodium thermal conductivity by Thurnay (1989). The thermal conductivity and viscosity of sodium vapor calculated by the extended function model are shown in Figs. 1 and 2, respectively, together with the data evaluated by Vargaftik and Yargin (1985).

The Leonard-Jones parameters are required to calculate the binary diffusion coefficient. For σ_{M}, we employ an average interaction distance of sodium atom (Iida and Guthrie, 1993), which is consistent with the value used by Grosse (1965) who calculated the sodium-vapor viscosity based on an ideal gas equation:

$\sigma_{\mathrm{M}} = 3.46$ Å.

The Leonard-Jones parameter ε_M is unknown and hence is estimated by means of the following empirical relation (Bird et al., 1960):

$$\varepsilon_M / k_B = 1.92 T_m , \qquad (55)$$

where T_m is the sodium melting point. The resultant value is

$$\varepsilon_M / k_B = 712 \text{ K}.$$

3.5. *Surface tension*

A. *Fuel*

The surface tension of liquid mixed oxide fuel is not known experimentally. For the surface tension of liquid UO_2, Fink and Petri (1997) recommended results of a critical review by Hall et al. (1987). The recommended surface tension of liquid UO_2 at the melting point is an average of several measurements with a temperature dependence estimated for the temperature range 3120 - 3225 K:

$$\sigma = 0.513 - 0.19 \times 10^{-3} (T - 3120), \qquad (56)$$

where σ is in J m^{-2} and T is in K. This equation is also recommended in the assessment by Harding et al (1989). The parameters in Eq. (31) are determined to give the same values of surface tension and the temperature coefficient (see Eq. (62)) with Eq. (56) at the melting point of UO_2. The resultant equation is

$$\sigma = 1.348 \left(1 - \frac{T}{T_{Crt}} \right)^{2.770}, \qquad (57)$$

where σ is in J m^{-2} and T is in K, and T_{Crt} is the critical temperature of UO_2 and mixed oxide (= 10600 K). The is used for both UO_2 and mixed oxide.

B. *Stainless steel*

The surface tension of type 316 stainless steel in liquid state is not known experimentally. Nikolopoulous and Schulz (1979) obtained the following linear relationship for the surface tension of type 1.4970 stainless steel:

$$\sigma = 1.19 - 0.57 \times 10^{-3} (T - 1690), \qquad 1690 \text{ K} < T < 1930 \text{ K}, \qquad (58)$$

where σ is in J m^{-2} and T is in K. This relationship was determined by melting cylindrical samples of type 1.4970 stainless steel on substrate material UO_2. An alternative measurement was performed by Ahmad and Murr (1976) in hydrogen atmosphere for type 304 stainless steel and on Al_2O_3 as substrate material. They obtained

$$\sigma = 1.172 - 8.24\times10^{-3}(T-1748),\quad 1748\ \mathrm{K} < T < 1773\ \mathrm{K}, \tag{59}$$

where σ is in J m^{-2} and T is in K. It is noted that the values calculated by both relationships agrees well at the liquidus temperature of type 316 stainless steel (= 1753 K), but the temperature coefficient differs by more than an order of magnitude. In addition, the temperature coefficients in Eqs. (58) and (59) seem to be too negative because Eqs. (58) and (59) become zero at 1890 K and 3778 K, respectively, which are too low as compared with the critical temperature of stainless steel (= 9600 K). These facts suggest that there is still large uncertainty in the surface tension of stainless steel in the high temperature region.

A well-known approximation between surface tension and temperature is give by Eötvös' law, which is expressed in the form (Allen, 1972; Iida and Guthrie, 1993)

$$\sigma = \frac{k}{(W\upsilon_l)^{2/3}}(T_{\mathrm{Crt}} - T), \tag{60}$$

where k is approximately equal to 6.4×10^{-8} (J K^{-1} mol$^{-2/3}$) for liquid metals (Grosse, 1962). By differencing Eq. (60) with respect to temperature, the temperature coefficient of surface tension is

$$\frac{\mathrm{d}\sigma}{\mathrm{d}T} = -\frac{\sigma}{T_{\mathrm{Crt}} - T}\left\{\frac{2(T_{\mathrm{Crt}} - T)}{3}\frac{\mathrm{d}\upsilon_l}{\mathrm{d}T} + 1\right\}. \tag{61}$$

Using known properties of type 316 stainless steel (Morita et al., 1998), the values of surface tension and temperature coefficient are calculated at its liquidus temperature:

$\sigma_{\mathrm{Liq}} = 1.265$ J m^{-2}, and

$$\left.\frac{\mathrm{d}\sigma}{\mathrm{d}T}\right|_{\mathrm{Liq}} = -\,0.238\times10^{-3}\ \mathrm{J\ m^{-2}\ K^{-1}}.$$

One should note that the above value of surface tension calculated through the use of Eötvös' law shows good agreement with the experimental data for stainless steel (Nikolopoulous and Schulz, 1979; Ahmad and Murr, 1976), and the temperature coefficient is also within the uncertainty of experimental values for liquid iron (Allen, 1972).

Equation (60) is a better approximation of the temperature coefficient near the melting point, and the van der Waals equation (31) gives a more realistic surface tension relation near T_{Crt} (Allen, 1985). The temperature coefficient from Eq. (31) is expressed by

$$\frac{\mathrm{d}\sigma_{\mathrm{Lm}}}{\mathrm{d}T_{\mathrm{Lm}}} = -\frac{c_{\mathrm{SL2,M}}\sigma_{\mathrm{Lm}}}{T_{\mathrm{Crt,M}} - T_{\mathrm{Lm}}}. \tag{62}$$

Comparison of Eqs. (61) and (62) results in

$$c_{\mathrm{SL2,M}} = 1 + \frac{2(T_{\mathrm{Crt}} - T)}{3}\frac{\mathrm{d}\upsilon_l}{\mathrm{d}T}. \tag{63}$$

This yields $c_{\mathrm{SL2,M}} = 1.48$ for type 316 stainless steel at its liquidus temperature. Consequently, for the stainless steel the surface tension and its temperature coefficient at the liquidus temperature calculated by Eötvös' law are used to determine the fitting constants in the van der Waals equation (31). The resultant equation is

$$\sigma = 1.704\left(1 - \frac{T}{T_{\mathrm{Crt}}}\right)^{1.477}, \tag{64}$$

where σ is in J m^{-2} and T is in K , and T_{Crt} is the critical temperature of stainless steel.

An equilibrium balance of the surface forces between solid and liquid with the contact angle θ can be expressed by the Young equation:

$$\sigma_{\mathrm{S}} = \sigma_{\mathrm{SL}} + \sigma_{\mathrm{L}}\cos\theta, \tag{65}$$

where σ_{L} is the surface tension of the liquid, σ_{S} is the surface tension of the solid, and σ_{SL} is the interfacial tension between the two. For the UO_2–stainless steel system, Nikolopoulous and Schulz (1979) measured the contact angle and the surface tension of type 1.4970 stainless steel, which is given by Eq. (58). Using the known surface tension of solid UO_2 (see Eq. (67)), they determined the interfacial tension between UO_2 and type 1.4970 stainless steel:

$$\sigma_{\mathrm{SL}} = 1.57 - 2.01\times10^{-3}(T - 1690), \tag{66}$$

where σ_{SL} is in J m^{-2} and T is in K. Eq. (66) yields a contact angle $\theta = 124°$ at the steel melting point, and $\theta = 0°$ (perfect wetting) at 2515 K. It is noted that this is consistent with the examination on the wetting and capillary properties of molten steel in contact with solid oxide fuel (Ostensen et al, 1977), that is, the molten stainless steel does not wet oxide fuel except at very high temperatures.

Now, we apply Eq. (64) to Eq. (65) for the UO_2–stainless steel system. Nikolopoulous et al. (1977) experimentally determined the following linear temperature function for the surface energy of UO_2:

$$\sigma_{\mathrm{S}} = 1507.0 - 0.3457T, \qquad 0\,\mathrm{K} < T < 3073\,\mathrm{K}, \tag{67}$$

where σ_{S} is in erg cm^{-2} and T is in K. Hall et al. (1987) reviewed measurements of the surface energy of UO_2 and gave the following correlation as a mean line with error of $\pm 70\%$:

$$\sigma_{\mathrm{S}} = 0.85 - 1.4\times10^{-4}T, \qquad 273\,\mathrm{K} < T < 3120\,\mathrm{K}, \tag{68}$$

where σ_{S} is in J m^{-2} and T is in K. Equations (67) and (68) yield 0.43 J m^{-2} and 0.45 J m^{-2}

at the melting point, respectively. However, it seems unreasonable to accept that the surface tension increases at the melting transition. Eberhart (1968) estimated the surface tension of solid UO_2 at the melting point from the surface tension of liquid UO_2 using the relation derived for metal, that is, $\sigma_S = 1.1\,\sigma_L$. Therefore, in consideration of the uncertainty in Eqs. (67) and (68), we assume 0.56 J m^{-2} for the surface tension of solid UO_2 at the melting point, which is calculated using Eq. (56), and then fit the experimental data of the surface tension of solid UO_2 by Nikolopoulous et al. (1977) using the lease squares method:

$$\sigma_S = 0.56 - 2.3\times10^{-4}(T - 3120), \tag{69}$$

where σ_S is in J m^{-2} and T is in K. This gives good agreement with the surface energy of the relaxed UO_2 surface for low temperature range (~300 ℃) suggested by Matzke et al. (1980), which would be in the range of 1.2 ± 0.3 J m^{-2}. Substituting Eqs. (64) and (69) into Eq. (65) and using the experimental data of the contact angle between UO_2 and type 1.4970 stainless steel (Nikolopoulous and Schulz, 1979), we can determine the interfacial tension between UO_2 and stainless steel. The least squares fitted line is given by

$$\sigma_{SL} = 1.60 - 1.99\times10^{-3}(T - 1690), \tag{70}$$

where σ_{SL} is in J m^{-2} and T is in K. This indicates the very good agreement with Eq. (66), and hence means that Eqs. (64) and (69), which seem to be physically reasonable, are consistent with available data of surface tensions in the UO_2–stainless steel system. Figure 3 shows the present results on the surface forces between solid and liquid in the UO_2–stainless steel system.

C. Sodium

Fink and Leibowitz (1996) recommended the values for the surface tension of liquid sodium calculated for the following equation:

$$\sigma = 0.2405\left(1 - \frac{T}{T_{Crt}}\right)^{1.126}. \tag{71}$$

where σ is in J m^{-2} and T is in K and T_{Crt} is the critical temperature of sodium (= 2503.7 K). This is based on the van der Walls equation given by Goldman (1984), but the parameters in his equation were adjusted consistently with the critical temperatures, 2503.7 K. The constants in Eq. (71) are directly used for Eq. (31).

3.6. Liquid heat capacity at constant pressure

A. Fuel

The heat capacity of molten UO_2 has been measured by Ronchi et al. (1993) in the temperature range from the melting point to 8000 K. They fit their data for the entire temperature range to the equation:

$$c_p = 277 + \frac{1.1\times10^7}{T^2}\exp\left(\frac{15500\pm1000}{T}\right) + \frac{1.0\times10^{12}}{T^2}\exp\left(-\frac{35500\pm4000}{T}\right), \tag{72}$$

where c_p is in J kg K^{-1} and T is in K. Recently, Fink and Petri (1997) reviewed the heat capacity data measured by Ronchi et al. (1993) and other enthalpy data available, and recommended the following equation for the heat capacity of liquid UO_2:

$$c_p = -0.31182 + \frac{4.9211\times10^9}{T^2}, \tag{73}$$

where c_p is in J kg K^{-1} and T is in K. It is noted that this data fit was limited to the temperature range 3120 to 4500 K, and it gives us more accurate heat capacity of liquid UO_2 below 4500 K. However, we employ Eq. (72) to fit Eq. (27)for both UO_2 and mixed oxide because higher temperature range is needed for fast reactor safety analysis and deviations of Eq. (72) from Eq. (73) below 4500 K are almost within the uncertainty range estimated by Fink and Petri (1997).

B. Stainless steel

The heat capacity of liquid stainless steel is not known experimentally. Here, the heat capacity at constant pressure of type 316 stainless steel in liquid state is evaluated using the thermodynamic relationships developed in our previous study (Morita and Fischer, 1998).

C. Sodium

Fink and Leibowitz (1996) calculated the heat capacity at constant pressure of liquid sodium using the following thermodynamic relationship:

$$c_p = \left(\frac{dh_l}{dT}\right)_{\mathrm{Sat}} + \frac{(T\alpha_p - 1)}{\rho_l}\left(\frac{dp}{dT}\right)_{\mathrm{Sat}}, \tag{74}$$

where the liquid density ρ_l, the partial derivatives $\left(\frac{dh_l}{dT}\right)_{\mathrm{Sat}}$ and $\left(\frac{dp}{dT}\right)_{\mathrm{Sat}}$, and the volumetric thermal expansion coefficient α_p are calculated from their recommended equations.

3.7. Code options and TPP functions

The analytic TPP model used for the calculation of liquid and vapor properties for a material with the material number M is controlled by the input option, KPOPT(N, M) for thermal conductivities and MUOPT(N, M) for viscosities, in the NAMELIST class, XTPP. Here N refers to the sub-material number. If KPOPT(N, M) = 1 or MUOPT(N, M) = 1, the properties of a material M with the sub-material number N are calculated using the simple analytical functions. If KPOPT(N, M) = 2 or MUOPT(N, M) = 2, the properties are calculated using the extended function model. Otherwise, the liquid properties are calculated using the simple function model alone and the vapor properties are theoretically evaluated. Sets of parameters used to calculate the thermophysical properties are specified by inputs in the NAMELIST classes, XTPP and XEOS. The TPP functions prepared for SIMMER-III are listed in Table 1. A complete set of parameters in the proposed TPP functions is presented in Tables 2-5 for the basic reactor-core materials: uranium dioxide, mixed-oxide fuel, stainless steel, and sodium. The TPP functions and parameters defined in the analytic TPP model are described in the previous chapters.

Chapter 4. Conclusions

The analytic TPP model was developed for the reactor safety analysis code SIMMER-III. This model using the general function forms is designed to be flexible sufficiently to represent correct behavior of material properties over wide temperature ranges. New formulation was proposed to calculate the thermal conductivity and viscosity of liquid and vapor phases. The equations for vapor and liquid have the consistency between liquid and vapor near the critical point, and for vapor the properties depend on the two variables, density and temperature. The analytical function set to calculate the thermophysical properties of the basic reactor-core materials was completed based on the most up-to-date and reliable data sources as well as new evaluations. Together with the previous studies on the thermodynamic properties and equations of state, the analytic TPP model developed in this study can be utilized as a standard basis for the fast reactor safety analysis.

Acknowledgments

The initial stage of this study was jointly performed under the agreement between the United States Nuclear Regulatory Commission and the Japan Nuclear Cycle Development Institute (JNC), which was formerly called the Power Reactor and Nuclear Fuel Development Corporation (PNC). The authors are grateful to W.R. Bohl of the Los Alamos National Laboratory for his significant contribution to forming the basis of SIMMER-III. The authors would also like to acknowledge the helpful discussions with D. J. Brear, who was the International Fellow of PNC, and N. Shirakawa of Toshiba. Special thanks are due to M. Sugaya of Marubeni Software for his significant assistance in programming and computation. The present study has been completed in collaboration with FZK under the SIMMER-III code development program at JNC.

Appendix A. Consistent formulation for thermal conductivity and viscosity

A.1. Review of Hanley's model

The only established theory to calculate vapor transport properties is the kinetic theory for low-density gases. It was used successfully by Hanley (1973) to calculate the viscosity and thermal conductivity of dilute argon, krypton, and xenon. The major deficiency in this theory is that it describes the properties dependent on temperature, but not on density, and is valid only for dilute gases. This means that increases in the thermal conductivity and viscosity due to the high density near the critical point are neglected. The increase, as compared to the dilute gas value, amounts typically to a factor of three or four for the viscosity, and for the thermal conductivity of nonmetal vapors. However, a drastic increase (~ two orders of magnitude) occurs for metal vapors, because the dense vapors show clear 'metallic' properties (high thermal and electrical conductivity) which are not present in dilute vapors. In analyses of processes such as fuel-coolant interactions or steam explosions, the coolant such as sodium and water may be predicted to reach temperature near the critical point. It is, therefore, necessary that properties of the coolant show the correct behavior near the critical point, especially that the vapor and liquid data are consistent at high densities. In this appendix, new formulation is proposed to calculate the thermal conductivity and the viscosity for the coolant materials, which can be used up to and beyond the critical temperature.

Hanley et al. (1974) included the density dependence in an evaluation of the viscosity and thermal conductivity for some simple gases (noble gases, nitrogen, and oxygen). Their approach is not based on a theoretical model. They used rather simple analytical functions, and adjusted them to experimental data. First, they obtained the following empirical function to represent experimental data:

for viscosity

$$\mu_g(\rho_g,T_g)=\mu_0(T_g)+\mu_1(T_g)\rho_g,\text{ and} \tag{A1}$$

for thermal conductivity

$$\kappa_g(\rho_g,T_g)=\kappa_0(T_g)+\kappa_1(T_g)\rho_g, \tag{A2}$$

where $\mu_0(T_g)$ and $\kappa_0(T_g)$ are the dilute gas values at a given temperature, which can be calculated by the kinetic theory for gases, and $\mu_1(T_g)$ and $\kappa^{D}(T_g)$ are defined as first density corrections. To improve the accuracy of the above correlations, they defined excess functions, which are simply the difference between averaged experimental data and the approximations, Eqs. (A2) and (A1). They also obtained equations for the excess functions, excluding the critical region. It is known that the thermal conductivity increases in the critical region. This critical point enhancement is calculated by a simple model, and is added to Eqs. (A2) and (A1) with the excess functions. At the critical point, this model gives the value

$$\Delta\kappa_c = k_B T_g^2 \left(\frac{\partial p}{\partial T}\right)_\rho^2 \beta_T^{1/2} Y, \qquad \text{(A3)}$$

with

$$Y = \left[6\pi\mu L \left(\frac{k_B T \rho N}{W}\right)^{1/2}\right]^{-1}, \qquad \text{(A4)}$$

where L is a length parameter of the order of the hard-sphere diameter.

We estimate the magnitude of the critical point enhancement of the sodium thermal conductivity using Eqs. (A3) and (A4). The following data from the recommendation by Fink and Leibowitz (1996) are used for the purpose of this estimate:

$$\left(\frac{dp}{dT}\right)_c = 4.689 \times 10^4 \text{ Pa},$$

$$\mu_c = 5.8 \times 10^{-5} \text{ Pa s},$$

$$\rho_c = 219 \text{ kg m}^3\text{, and}$$

$$\beta_T = 8.885 \times 10^{-6} \text{ Pa}^{-1} \text{ at } 2500 \text{ K}.$$

The length parameter L is taken from the Lennard-Jones parameter σ used by Grosse (1965):

$$L = 3.46 \text{ Å}.$$

As the result, Eq. (A3) yields

$$\Delta\kappa_c = 0.106 \text{ W m}^{-1} \text{ K}^{-1}.$$

This is small compared to the rather large metallic conductivity near the critical point, 5 W m^{-1} K^{-1} by Thurnay (1981), 5.16 W m^{-1} K^{-1} by Fink and Leibowitz (1982), and 1.8 W m^{-1} K^{-1} by Bystrov et al. (1990), although Fink and Leibowitz (1996) recommended 0.052 W m^{-1} K^{-1} in their resent assessment, which was simply obtained from extrapolation of the thermal conductivity evaluated by Vargaftik and Yargin (1985). It is noted, however, that the critical point enhancement is not numerically small for water, but only in a small range around the critical point.

A.2. Proposed model

We follow essentially the method of Hanley et al. (1974), but for simplicity neglect both small excess functions and the critical point enhancement of the thermal conductivity. It is proposed to use equations of the type (A2) and (A1) and a simple power function for κ_1 and μ_1

below the critical temperature, and a constant value above. As the result, we obtain the following equations for the gas side:

$$\kappa_g(\rho_g,T_g)=\kappa^D(T_g)+\left[\kappa_c-\kappa^D(T_c)\right]\left(\frac{T_g}{T_c}\right)^x\frac{\rho_g}{\rho_c},\ \text{and} \tag{A5}$$

$$\mu_g(\rho_g,T_g)=\mu^D(T_g)+\left[\mu_c-\mu^D(T_c)\right]\left(\frac{T_g}{T_c}\right)^x\frac{\rho_g}{\rho_c}, \tag{A6}$$

where κ^D and μ^D refer to the thermal conductivity and the viscosity of dilute gas, respectively. It is noted that Hanley et al. (1974) proposed a different function for κ_1 and μ_1, that is,

$$\kappa_1,\ \mu_1 \sim A+B(C-\ln T^*)^2, \tag{A7}$$

where A, B, and C are fitting parameters, and T^* is the reduced temperature, $T^*=k_BT_g/\varepsilon$. For this work, we prefer the simpler functions given in Eqs. (A5) and (A6), for several reasons. First, though Eq. (A7) shows the correct behavior around the critical temperature, the asymptotic behavior (for both low and high temperatures) is probably wrong; at least, it is not established to be correct. Second, at temperatures significantly below critical, the density dependence is unimportant, and it seems appropriate to require that the function κ_1 and μ_1 should decrease to zero. Third, for the material of major interest, sodium vapor, no data exist that would justify a 3-parameter approximation. The dilute gas values in Eqs. (A5) and (A6) can be calculated by the kinetic theory for simple gases (see Section 2.2.3). For more complex gases, e.g. for sodium vapor where a chemical reaction occurs, it is preferable to use linear equations of the type

$$\kappa^D=a_1+a_2T_g,\ \text{and} \tag{A8}$$

$$\mu^D=b_1+b_2T_g, \tag{A9}$$

which can be fitted to experimental or theoretical data.

On the liquid side, a quadratic equation is used for the thermal conductivity

$$\kappa_l=a_{l,1}+a_{l,2}T_l+a_{l,3}T_l^3, \tag{A10}$$

and the Andrade equation for the viscosity

$$\mu_l=b_{l,1}\exp\left(\frac{b_{l,2}}{T_l}\right). \tag{A11}$$

Both equations usually represent experimental data quite well over a wide temperature range. They have, however, the drawback that they have a finite slope at the critical point. It is, therefore, suggested to replace them near the critical point by equations of the type

$$\kappa_l = \kappa_c + a_{l,5}(T_c - T_l)^{1/2} + a_{l,6}(T_c - T_l)^2, \qquad a_{l,4}T_c < T_l \le T_c \tag{A12}$$

$$\mu_l = \mu_c + b_{l,4}(T_c - T_l)^{1/2} + b_{l,5}(T_c - T_l)^2. \qquad b_{l,3}T_c < T_l \le T_c \tag{A13}$$

Equations (A10) and (A11) should be used blow the temperatures $a_{l,4}T$ and $b_{l,3}T_c$, respectively.

A.3. Application to water

For the calculation of the water transport properties, we apply the data from the steam tables (Haar et al., 1984). Equations (A10) and (A11) are fitted to the data of saturated water over the whole liquid temperature range for the liquid thermal conductivity and viscosity, respectively. The thermal conductivity at the critical temperature is evaluated as the average value of the saturated liquid and vapor at 600 K because the steam tables have no critical value of thermal conductivity. For the viscosity at the critical temperature, we apply the value from the steam tables. The parameters in Eqs. (A12) and (A13) are determined so as to satisfy the continuity condition at 600 K. For the vapor phase, Eqs. (A8) and (A9) are fitted to the data of saturated steam up to 375 K in the liquid temperature range. Using this temperature range, the temperature- and density-dependent functions, Eqs. (A5) and (A6) better represent the data on the saturation line if we use $x = 1$. As the result, we obtain the following expression:

for the thermal conductivity

$$\kappa_l = -0.280570 + 4.63990\times10^{-3}T_l - 5.57360\times10^{-6}T_l^3,$$

$$T_l \le 600\ \mathrm{K}, \tag{A14}$$

$$\kappa_l = \kappa_c + 3.02036\times10^{-2}(T_c - T_l)^{1/2} - 1.60687\times10^{-6}(T_c - T_l)^2,$$

$$600\ \mathrm{K} < T_l \le T_c, \tag{A15}$$

$$\kappa^D = -5.51710\times10^{-3} + 8.11940\times10^{-5}T_g, \tag{A16}$$

$$\kappa_g(\rho_g, T_g) = \kappa^D(T_g) + \left[\kappa_c - \kappa^D(T_c)\right]\frac{T_g\rho_g}{T_c\rho_c}, \text{ and} \tag{A17}$$

$$\kappa_c = 0.293100\ \mathrm{W\,m^{-1}\,K^{-1}},$$

for the thermal conductivity

$$\mu_l = -5.8915\times10^{-6}\exp\left(\frac{1487.6}{T_l}\right), \qquad T_l \le 600\ \mathrm{K}, \tag{A18}$$

$$\mu_l = \mu_c + 4.75264\times10^{-6}(T_c - T_l)^{1/2} - 5.90333\times10^{-10}(T_c - T_l)^2,$$

$$600\,\mathrm{K} < T_l \leq T_c, \tag{A19}$$

$$\mu^{D} = 6.8707\times10^{-7} + 3.0921\times10^{-8}T_g, \tag{A20}$$

$$\mu_g(\rho_g, T_g) = \mu^{D}(T_g) + \left[\mu_c - \mu^{D}(T_c)\right]\frac{T_g\rho_g}{T_c\rho_c}, \text{ and} \tag{A21}$$

$$\mu_c = 3.89900\times10^{-5}\,\mathrm{Pa\ s},$$

where κ is in W m^{-1} K^{-1}, μ is in Pa s, T is in K, and T_c = 647.126 K. The results are shown in Fig. 4 for the thermal conductivity and in Fig. 5 for viscosity, compared with the data from the steam tables.

Appendix B. Nomenclature

c_p, c_v	heat capacities at constant pressure, constant volume (J kg^{-1} K^{-1})
D_{ij}	binary diffusion coefficient for species i and j (m^2 s^{-1})
D_{im}	effective binary diffusivity for the diffusion of i in a mixture (m^2 s^{-1})
e	specific internal energy (J kg^{-1})
f_D	correction factor close to unity in Eq. (21)
k_B	Boltzmann's constant (J K^{-1})
N	Avogadro's number
n	number density of molecules in a mixture
p	pressure (Pa)
R_m	gas constant (J mol^{-1} K^{-1})
T	temperature (K)
W	molecular weight (kg mol^{-1})
x_i	mole fraction of a component i in the mixture

Greek letters

α_p	volumetric thermal expansion coefficient (K^{-1})
β_S	adiabatic compressibility (Pa^{-1})
β_T	isothermal compressibility (Pa^{-1})
ε_{ij}	maximum attractive energy between two molecules (J)
ε_M	fractional porosity of solid fuel
κ	thermal conductivity (W m^{-1} K^{-1} or cal cm^{-1} s^{-1} K^{-1})
μ	viscosity (Pa s)
v_S	speed of sound (m s^{-1})
ρ	density (kg m^{-3})
σ	surface tension (N m^{-1})
σ_{ij}, σ_M	collision diameter (Å)
Ω_D, $\Omega_\mathrm{k,m}$	collision integral
v	specific volume (m^3 kg^{-1})

Subscripts

Crt, c	critical point
G, g	vapor mixture
Gm	material component m in vapor field
Liq	liquidus point
Lm, Lm'	energy component m in liquid field
l	liquid
M	material number
m	melting point
N	sub-material number
Sat	saturation
Sm	energy component m in structure field
Vap	saturated vapor

Superscripts

D	dilute vapor

References

Ahmad, U.M., Murr, L.E., 1976. Surface free energy of nickel and stainless steel at temperatures above the melting point, J. Mat. Sci. 11, 224–230.

Allen, B.C., 1972. The surface tension of liquid metals. In: Beer, S.Z. (Ed.), Liquid Metals, chemistry and physics, Chapter 4, Marcel Dekker, New York, pp. 161–212.

Allen, B.C., 1985. Surface tension. In: Ohse, R.W. (Ed.), Handbook of Thermodynamic and Transport Properties of Alkali Metals, Chapter 6.8, Blackwell Scientific Publications, Oxford, pp. 691–700.

Bird, R.B., Stewart, W.E., Lightfoot, E.N, 1960. Transport Phenomena, John Wiley & Sons, New York.

Bober, M. Breitung, W., Fischer, E.A., Schultz, B., Schumacher, G., 1983. Materialdaten von Geschmolzenen Kernbrennstoffen und Kernschmelzen für Störfallanalysen, KfK-Nachr. Jahrg. 15, 3/83, pp. 254–261.

Bystrov, P.I., Kagan, D.N., Krechetova, G.A., Shipil'rain, E.E., 1990. Liquid-Metal Coolants for Heat Pipes and Power Plants (Kirillin, V.A., Ed.), Hemisphere Pub. Corp., New York.

Chawla, T.C., Graff, D.L., Borg, R.C., Bordner, G.L., Weber, D.P., Millaer, D., 1981. Thermophysical properties of mixed oxide fuel and stainless steel type 316 for use in transition phase analysis, Nucl. Eng. Des. 67, 57–74.

Carey, V.P., 1992. Liquid-Vapor Phase-Change Phenomena: An Introduction to the Thermophysics of Vaporization and Condensation Processes in Heat Transfer Equipment, Hemisphere Pub. Corp., Washington.

Eberhart, J.G., 1968. The critical surface tension of uranium dioxide, J. Nucl. Mater. 25, 103–105.

Fink, J.K., Leibowitz, L., 1982. Calculation of thermophysical properties of sodium, in Sengers, J.V. (Ed.), Proceedings of the Eighth Symposium on Thermophysical Properties Vol. II: Thermophysical properties of solid and of selected fluids for energy technology, ASME, New York, pp. 165–173.

Fink, J.K., Leibowitz, L., 1985. An analysis of measurements of the thermal conductivity of liquid urania, High Temp.–High Pressures 17, 17–26.

Fink, J.K., Leibowitz, L., 1996. A consistent assessment of the thermophysical properties of sodium, High Temp. Mater. Sci. 35, 65–103.

Fink, J.K., Petri, M.C., 1997. Thermophysical Properties of Uranium Dioxide, ANL/RE-97/2, Argonne National Laboratory, February 1997.

Frurip, D.J., Fink, J.K., 1982. The thermal conductivity of UO_2 vapor, J. Nucl. Mater. 110, 309-316.

Goldman J.H., 1984. Surface tension of sodium, J. Nucl. Mater., 126, 86–88.

Grosse, A.V., 1962. The relationship between the surface tensions and energies of liquid metals and their critical temperatures, J. Inorg. Nucl. Chem. 27, 147–156.

Grosse, A.V., 1965. Viscosities of liquid sodium and potassium from their melting points to their critical points, Science 147, 1438–1441.

Haar, L., Gallagher, J.S., Kell, G.S., 1984. NBS/NRC Steam Tables, Hemisphere, New York.

Hall, R.O.A., Mortimer, M.J., Mortimer, D.A., 1987. Surface energy measurements on UO_2, A critical review, J. Nucl. Mater. 148, 237–256.

Hanley, H.J.M., 1973. The viscosity and thermal conductivity coefficients of dilute argon, krypton, and xenon, J. Phys. Chem. Ref. Data. 2, 619–642.

Hanley, H.J.M., McCarty, R.D., Haynes, W.M., 1974. The viscosity and thermal conductivity coefficients of dense gaseous and liquid argon, krypton, xenon, nitrogen, and oxygen, J. Phys. Chem. Ref. Data. 2, 979–1018.

Harding, J.H., Martin, D.G., 1989. A recommendation for the thermal conductivity of UO_2, J. Nucl. Mater. 166, 223–226.

Harding, J.H., Martin, D.G., Potter, P.E., 1989. Thermophysical and thermodynamic properties of fast reactor materials, Commission of the European Communities, EUR 12402 EN.

Iida, T., Guthrie, R.I.L., 1993. The Physical Properties of Liquid Metals, Clarendon Press, Oxford.

Kim, C.S., Haley, R.A., Fischer, J., Chasanov, M.G., Leibowitz, L., 1977. Measurement of thermal diffusivity of molten UO_2, in Cezairliyan, A. (Ed.), Proceedings of the Seventh Symposium on Thermophysical Properties, ASME, New York, pp. 338–343.

Kondo, Sa., Tobita, Y., Morita, K., Shirakawa, N., 1992. SIMMER-III: An advanced computer program for LMFBR severe accident analysis, Proceeding of the International Conference on Design and Safety of Advanced Nuclear Power Plant (ANP '92), Vol. IV, Tokyo, Japan, 25-29 October, 1992, pp. 40.5-1–40.5-11.

Matzke, Hj., Inoue, T., Warren, R., 1980. The surface energy of UO_2– as determined by Hertzian indentation, J. Nucl. Mater. 91, 205–220.

Morita, K., Fischer, E.A., 1998. Thermodynamic properties and equations of state for fast reactor safety analysis Part I: Analytic equation-of-sate model, Nucl. Eng. Des. 183, 177–191.

Morita, K., Fischer, E.A., Thurnay, K., 1998. Thermodynamic properties and equations of state for fast reactor safety analysis Part II: Properties of fast reactor materials, Nucl. Eng. Des. 183, 193–211.

Neufeld, P.D., Janzen, A.R., Aziz, R.A., 1972. Empirical equations to calculate 16 of the transport collision integrals $\Omega^{(l,s)*}$ for the Lennard-Jones (12–6) potential, J. Chem. Phys. 52, 1100–1102.

Nikolopoulous, P., Nazaré, S., Thümmler, F., 1977. Surface, grain boundary and interfacial energies in UO_2 and UO_2–Ni, J. Nucl. Mater. 71, 81–94.

Nikolopoulous, P., Schulz, B., 1979. Density, thermal expansion of stainless steel and interfacial properties of UO_2–stainless steel above 1690 K, J. Nucl. Mater. 82, 172–178.

Ostensen, R.W., Murphy, W.F., Wrona, B.J., Deitrich, L.W., Florek, J.C., 1977. Intrusion of molten steel into cracks in solid fuel in a transient-undercooling accident in a liquid-metal fast breeder reactor, Nucl. Tech, 36, 200–214.

Otter, C., Damien, D., 1984. Mesure de la diffusivité thermique de UO_2 fondu, High Temp.–High Pressures 16, 1–6.

Philipponneau, Y., 1992. Thermal conductivity of (U, Pu)O_{2-x} mixed oxide fuel, J. Nucl. Mater. 188, 194–197.

Reid, R.C., Prausnitz, J.M., Poling, B.E., 1988. The properties of Gases and Liquids, Fourth edition, McGraw-Hill, New York.

Ronchi, C., Hiernaut J.P., Selfslag, R., 1993. Laboratory measurement of the heat capacity of urania up to 8000 K: I. Experiment, Nucl. Sci. Eng. 113, 1–19.

Shipil'rain, E.E., Yakimovich, K.A., Fomin, V.A., Skovorodjko, S.N., Mozgovoi, A.G., 1985. Dynamic and kinetic viscosity of liquid alkali metals. In: Ohse, R.W. (Ed.), Handbook of Thermodynamic and Transport Properties of Alkali Metals, Chapter 7.3, Blackwell Scientific Publications, Oxford, pp. 753–784.

Tasman, H.A., Pel, D., Richter, J., Schmidt, H-E., 1983. Measurement of the thermal conductivity of liquid UO_2, High Temp.–High Pressures 15, 419–431.

Tasman, H.A., 1989. Thermal conductivity of liquid UO_2, Commission of the European Communities, EUR 12385, pp. 80–91.

Thurnay, K., 1981. Thermophysical Properties of Sodium in the Liquid and Gaseous States, KfK 2863, Kernforschungszentrum Karlsruhe, February 1981.

Thurnay, K., 1989. SODIUM, A Code for Calculating Thermophysical Properties of the Sodium in the Liquid and Gaseous States, KfK 4609, Kernforschungszentrum Karlsruhe, September 1989.

Vargaftik, N.B., Yargin, V.S., 1985. Thermal conductivity and viscosity of the gaseous phase. In: Ohse, R.W. (Ed.), Handbook of Thermodynamic and Transport Properties of Alkali Metals, Chapter 7.4, Blackwell Scientific Publications, Oxford, pp. 785–842.

Wilke, C.R., 1950. Diffusional properties of multicomponent gases, Chem. Eng. Prog. 46, pp. 95–104.

Woodley, R.E., 1974. The viscosity of molten uranium dioxide, J. Nucl. Mater. 50, 103–106.

Table 1. TPP functions for SIMMER-III.

Functions

XAPPLM (M, N, T)	:	Liquid heat capacity at constant pressure
XCPLM (M, N, T)	:	Vapor heat capacity at constant pressure
XDIFG (N1, M1, P1, N2, M2, P2, T)	:	Diffusion coefficient for binary system
XKPSM (M, N, T, EPF)	:	Solid thermal conductivity
XKPLM (M, N, T)	:	Liquid thermal conductivity
XKPGM (M, N, T, V)	:	Vapor thermal conductivity
XKPG (N, T, V1, V2, V3, V4)	:	Thermal conductivity of vapor mixture
XMULM (M, N, T)	:	Liquid viscosity
XMUGM (M, N, T, V)	:	Vapor viscosity
XMUG (N, T, V1, V2, V3, V4)	:	Viscosity of vapor mixture
XSGML (M, N, T)	:	Surface tension of liquid

Arguments

EPF	:	Fractional porosity of solid fuel
M	:	Material number
M1	:	Material number of component 1
M2	:	Material number of component 2
N	:	Sub-material number
N1	:	Sub-material number of component 1
N2	:	Sub-material number of component 2
P1	:	Partial pressure of vapor component 1 (Pa)
P2	:	Partial pressure of vapor component 2 (Pa)
T	:	Temperature (K)
V	:	Specific volume (m^3 kg^{-1})
V1	:	Specific volume of vapor material component 1 (m^3 kg^{-1})
V2	:	Specific volume of vapor material component 2 (m^3 kg^{-1})
V3	:	Specific volume of vapor material component 3 (m^3 kg^{-1})
V4	:	Specific volume of vapor material component 4 (m^3 kg^{-1})

Table 2. TPP parameters for fuel (UO_2).

```
(M=1, N=2)
(KPOPT(2,1)=1, MUOPT(2,1)=0)
 AKPS1= 2.02070E+00   AKPS2= 4.68440E+03   AKPS3=-1.04430E+06
 AKPS4=-2.60310E-03   AKPS5= 8.93780E-07
 AKPL1= 2.50000E+00   AKPL2= 0.00000E+00   AKPL3= 0.00000E+00
 AKPG1= 2.74937E+02   AKPG2=-3.19190E+05   AKPG3=-8.96730E-02
 AKPG4= 1.28610E-05   AKPG5=-6.79170E-10
 TMAX = 6.00000E+03
 BMUL1= 9.88000E-04   BMUL2= 4.62000E+03
 CSGL1= 1.34800E+00   CSGL2= 2.77000E+00   CSGL3= 2.56608E-02
 DCPL1= 1.12590E-01   DCPL2=-5.35780E-01   DCPL3= 8.45640E-01
 DCPL4=-9.71270E-01   DCPL5= 9.60050E-01   DCPL6=-4.42520E-01
 CPMAX= 1.00000E+04
 EPSM = 5.69400E+03   SIGM = 4.03000E+00   NATOM= 3
```

Table 3. TPP parameters for fuel (MOX).

```
(M=1, N=1)
(KPOPT(1,1)=1, MUOPT(1,1)=0)
 AKPS1= 3.69720E+00   AKPS2= 5.17160E+02   AKPS3= 8.35470E+03
 AKPS4=-2.29210E-03   AKPS5= 7.17150E-07
 AKPL1= 2.50000E+00   AKPL2= 0.00000E+00   AKPL3= 0.00000E+00
 AKPG1= 2.74937E+02   AKPG2=-3.19190E+05   AKPG3=-8.96730E-02
 AKPG4= 1.28610E-05   AKPG5=-6.79170E-10
 TMAX = 6.00000E+03
 BMUL1= 9.88000E-04   BMUL2= 4.62000E+03
 CSGL1= 1.34800E+00   CSGL2= 2.77000E+00   CSGL3= 2.64185E-02
 DCPL1= 1.12590E-01   DCPL2=-5.35780E-01   DCPL3= 8.45640E-01
 DCPL4=-9.71270E-01   DCPL5= 9.60050E-01   DCPL6=-4.42520E-01
 CPMAX= 1.00000E+04
 EPSM = 5.69400E+03   SIGM = 4.03000E+00   NATOM= 3
```

Table 4. TPP parameters for steel (type 316 stainless steel).

(M=2, N=1)

(KPOPT(1,2)=1, MUOPT(1,2)=0)

AKPS1= 9.73500E+00	AKPS2= 0.00000E+00	AKPS3= 0.00000E+00
AKPS4= 1.43400E-02	AKPS5= 0.00000E+00	
AKPL1= 1.09810E+01	AKPL2= 3.21400E-03	AKPL3= 0.00000E+00
AKPG1=-1.93570E+00	AKPG2=-2.38340E+03	AKPG3=-8.71460E-05
AKPG4= 8.71000E-08	AKPG5=-7.10690E-12	
TMAX = 6.00000E+03		
BMUL1= 2.93000E-05	BMUL2= 9.71500E+03	
CSGL1= 1.7040E+00	CSGL2= 1.47700E+00	CSGL3= 6.32561E-02
DCPL1= 1.19300E-02	DCPL2= 1.43520E-02	DCPL3=-9.72070E-02
DCPL4= 1.94770E-01	DCPL5=-1.94480E-01	DCPL6= 7.20490E-02
CPMAX= 1.00000E+04		
EPSM = 3.26400E+03	SIGM = 2.41400E+00	NATOM= 1

Table 5. TPP parameters for coolant (sodium).

(M=3, N=1)

(KPOPT(1,3)=2, MUOPT(1,3)=2)

AKPL1= 1.01350E+02	AKPL2=-4.87840E-02	AKPL3= 4.24470E-06
AKPL4= 7.98818E-01	AKPL5= 4.50954E-01	AKPL6= 2.15988E-05
AKPG1= 2.31640E-02	AKPG2= 1.99610E-05	
BMUL1= 6.75520E-05	BMUL2= 9.23790E+02	BMUL3= 7.98818E-01
BMUL4= 2.55308E-06	BMUL5=-3.18826E-11	
BMUG1= 1.23750E-05	BMUG2= 4.48280E-09	
KPCRT= 5.16000E+00	MUCRT= 5.80000E-05	NF = 1
CSGL1= 2.40500E-01	CSGL2= 1.12600E+00	CSGL3= 1.00382E-02
DCPL1= 1.13560E-02	DCPL2=-3.29160E-02	DCPL3= 3.38130E-02
DCPL4=-1.52410E-02	DCPL5= 2.28360E-03	DCPL6= 1.36020E-03
CPMAX= 1.00000E+04		
EPSM = 7.12000E+02	SIGM = 3.46000E+00	

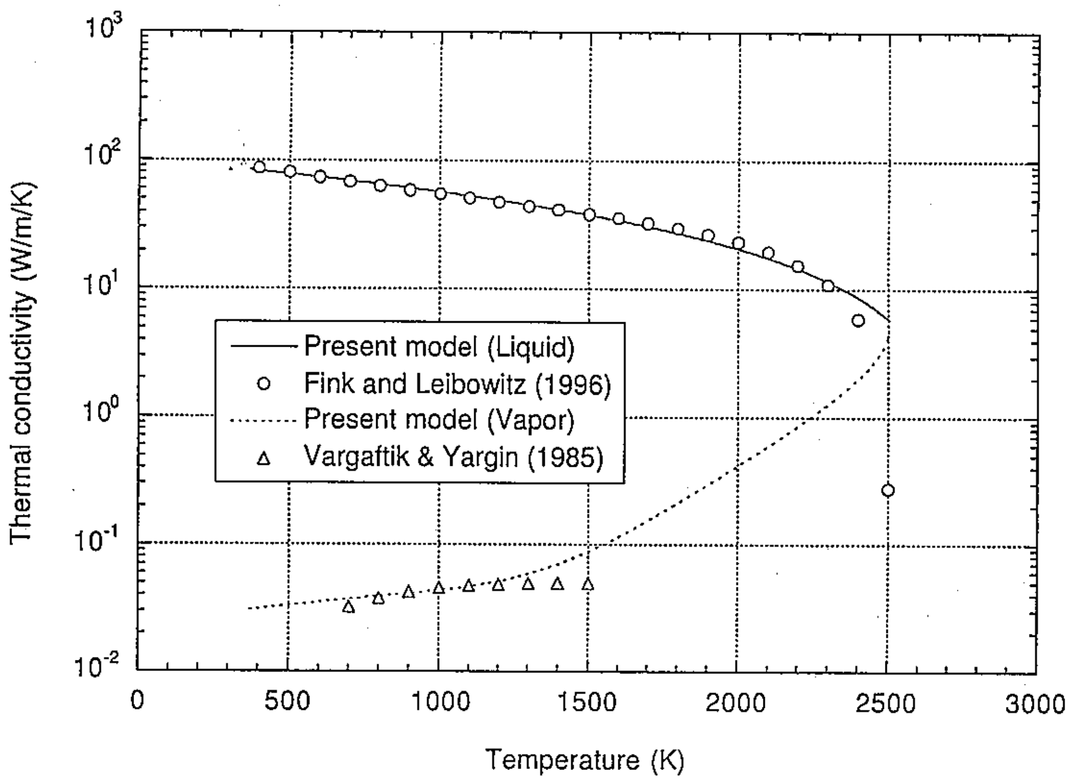

Fig. 1. Thermal conductivity of sodium.

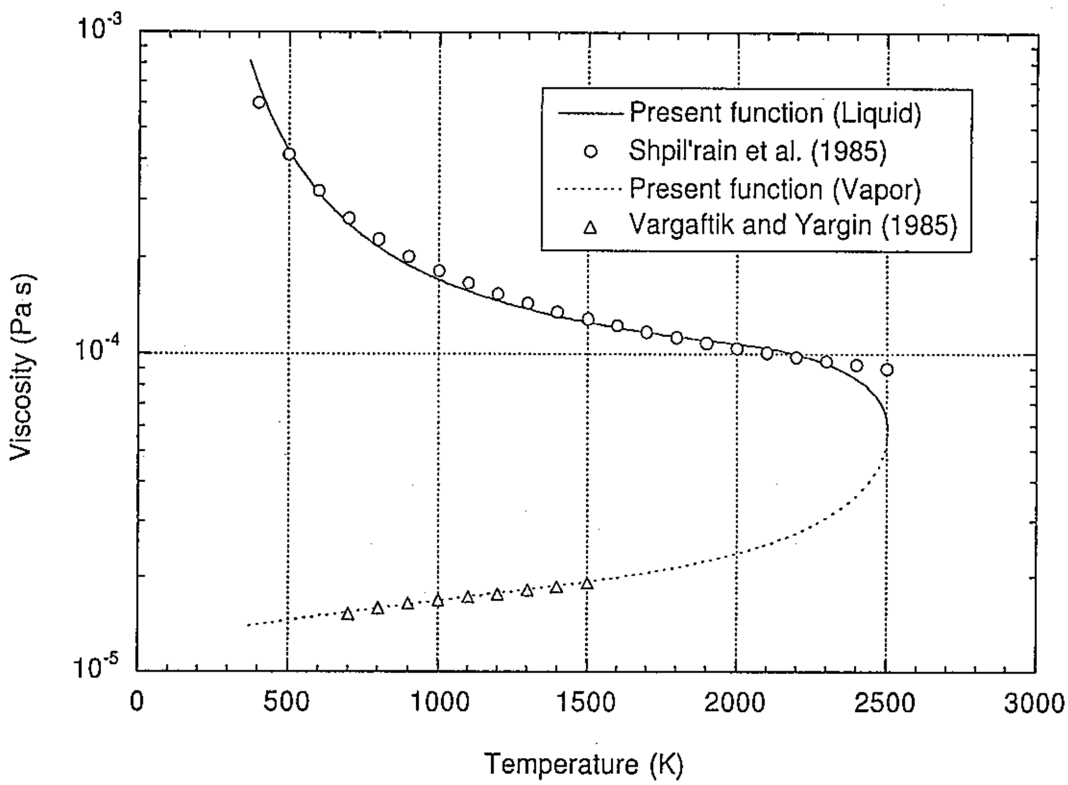

Fig. 2. Viscosity of sodium.

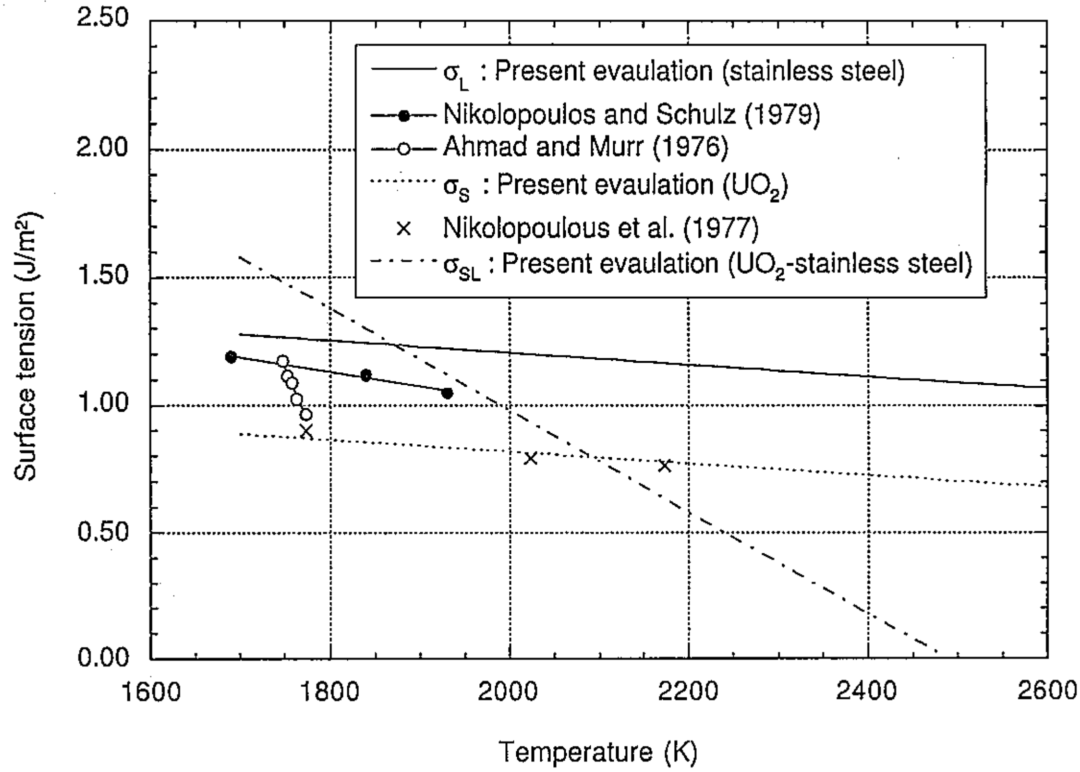

Fig. 3. Surface forces in UO_2–stainless steel system.

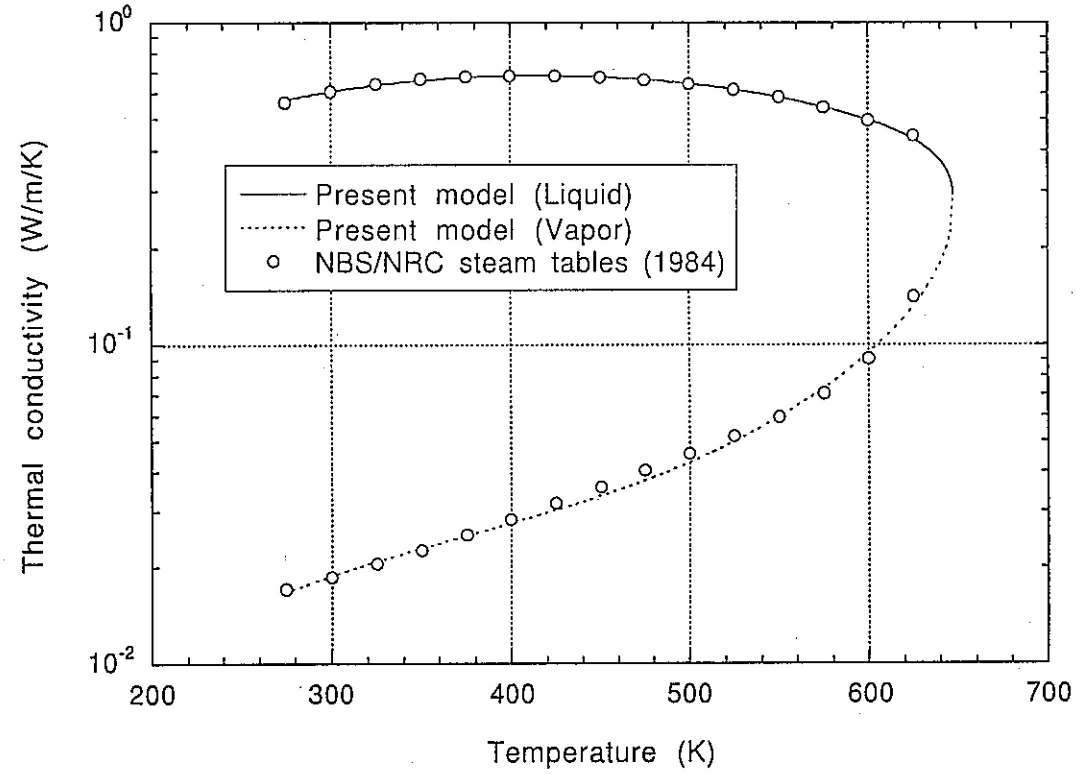

Fig. 4. Thermal conductivity of water.

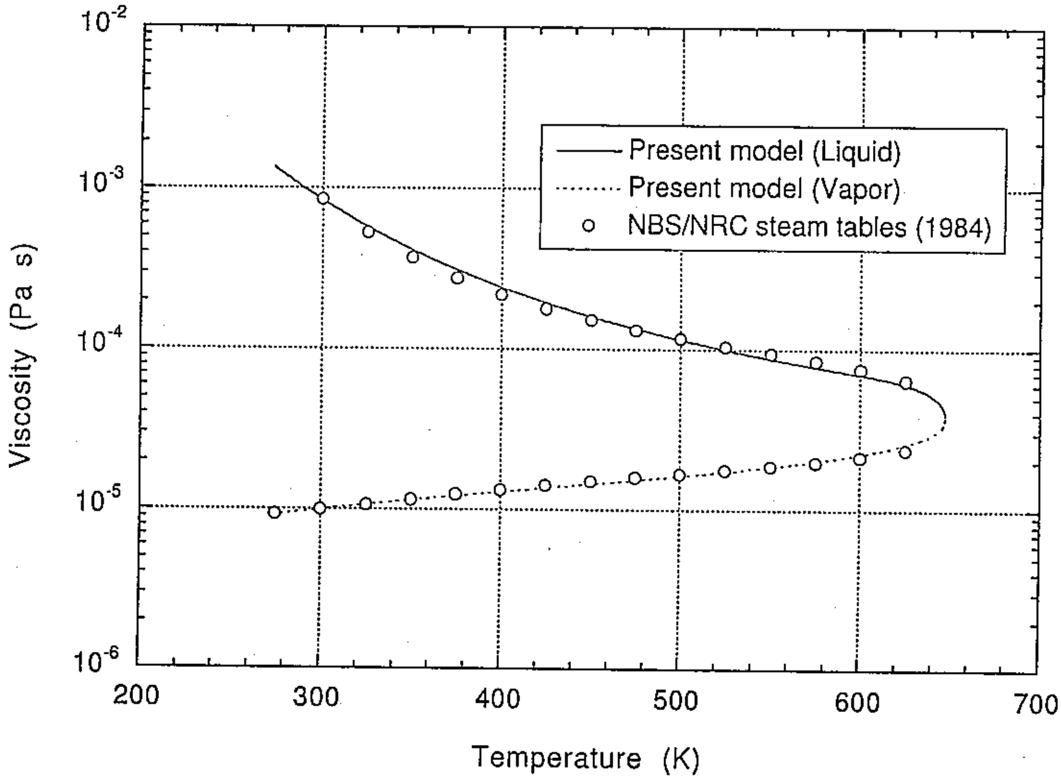

Fig. 5. Viscosity of water.